Initial Stages in Zirconia Coatings Using ESD

Roberto Neagu, Dainius Perednis, Agnès Princivalle, and Elisabeth Djurado*

Laboratoire d'Electrochimie et de Physico-Chimie des Matériaux et des Interfaces, ENSEEG-INPG/UJF/CNRS, 1130, rue de la Piscine, Domaine Universitaire, 38402 St. Martin d'Hères, France

Received September 22, 2004. Revised Manuscript Received December 6, 2004

This study describes the phenomena occurring during the first stages of layer formation in the ESD (electrostatic spray deposition) process. Solutions containing zirconyl nitrate dissolved in a mixture of butyl carbitol−water−ethanol (40:40:20 vol %) have been sprayed on heated glass substrates. The spreading and drying of the droplets and the growth of the coating over a time range of 10 s to 10 min have been studied using SEM and optical microscopy. The influence of the substrate temperature, concentration of the salts, nature, and concentration of polymer additives on the microstructure of the deposited coatings has been studied. This work shows that there is little connection between the evolution of the droplets spreading and the final microstructure of the coating. This is due to the strong effect of the preferential landing and to the presence of a liquid layer at the surface of the coating during the deposition process. These results will contribute to the understanding of the coating formation in the ESD technique. They will finally help to synthesize finely controlled thin layers of zirconia for direct applications as SOFC electrolytes.

Introduction

There are many processes that occur either sequentially or simultaneously during film formation by spray pyrolysis. These processes include precursor solution atomization, droplet transport and evaporation, impact of droplet and spreading on the substrate, and drying and decomposition of the precursor salt. If an electrical field is used to atomize the precursor solution and the resulted spray is used for film deposition, the technique is called electrostatic spray deposition (ESD). The control of the film quality requires a good understanding of the whole ESD process, beginning with its first stage, the spreading of the droplets onto the substrate. The impact of a droplet onto a substrate is a complex phenomenon. It is dependent on several factors including droplet size, impact velocity, and solvent and substrate surface properties.

Bussmann et al.[1] have compared experimental and simulated results on droplet impact on a solid surface. On impact, as a droplet reacts to a pressure increase, an axisymmetric film of liquid begins to spread on the surface. Dramatic influence of surface roughness was observed. The impact onto the smoothest surface typically gives an axisymmetric, regular shape. On rougher surfaces, regular undulations of the fluid surface evolve into finger-shaped splat border after the impact. This last phenomenon is called "fingering".

Pasandideh-Fard et al.[2] observed that the addition of a surfactant did not affect droplet shape during the initial stages of the spreading but has increased the maximum spread diameter and reduced recoil height. Indeed, the equilibrium contact angles were reduced by surfactant addition.

Sikalo et al.[3] studied the influence of various impact parameters on the droplet spreading, such as surface material, impact velocity, viscosity, surface tension, and droplet size. A droplet with high viscosity produces a smaller maximum spread. Moreover, it approaches its maximum spread in a shorter time. The maximum spread increases with decreasing contact angle. The authors suggested that viscosity effects are relatively more important to the smaller droplets and surface tension effects are relatively more important to the larger droplets.

Oh et al.[4] have experimentally and theoretically investigated the formation of a TiO_2 film by chemical aerosol deposition. Viscosity and surface tension are the forces that limit the spreading and bring the fluid to an equilibrium configuration.

Generally, the spreading of a droplet is described as a succession of intermediate steps. The number of steps, the shape of the liquid surface during spreading, and the size of the final splat depend on the size and velocity of the droplet, properties of the liquid (viscosity, surface tension), and the contact angle between the substrate and the liquid. Figure 1 shows a possible sequence from the impacting droplet to the equilibrium meniscus.

The spreading of a liquid droplet on a flat, smooth surface at different substrate temperatures has also been extensively studied and modeled.[1,4−11] When heat transfer between the

* Author to whom correspondence should be addressed. Phone: +33-4-76826684; fax: +33-4-76826777; e-mail: Elisabeth.Djurado@lepmi.inpg.fr.

(1) Bussmann, M.; Chandra, S.; Mostaghimi, J. *Phys. Fluids* **2000**, *12*, 3121.
(2) Pasandideh-Fard, M.; Qiao, Y. M.; Chandra, S.; Mostaghimi, J. *Phys. Fluids* **1996**, *8*, 650.
(3) Sikalo, S.; Marengo, M.; Tropea, C.; Ganic, E. N. *Exp. Thermal Fluid Sci.* **2002**, *25*, 503.
(4) Oh, E. K.; Kim, S. G. *J. Aerosol Sci.* **1996**, *27*, 1143.
(5) Harvie Dalton, J. E.; Fletcher David, F. *Int. J. Heat Mass Transfer* **2001**, *44*, 2633.
(6) Harvie Dalton, J. E.; Fletcher David, F. *Int. J. Heat Mass Transfer* **2001**, *44*, 2643.
(7) Zhao, Z.; Poulikakos, D.; Fukai, J. *Int. J. Heat Mass Transfer* **1996**, *39*, 2771.
(8) Zhao, Z.; Poulikakos, D.; Fukai, J. *Int. J. Heat Mass Transfer* **1996**, *39*, 2791.

10.1021/cm048341p CCC: $30.25
Published on Web 01/22/2005

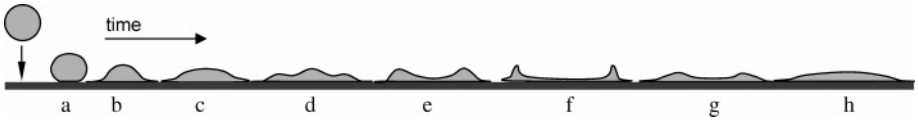

Figure 1. Spreading of a liquid droplet onto a flat, smooth, solid surface.

spreading droplet and the surface occurs, additional phenomena may be present: liquid heating or cooling, solvent vaporization, and precipitation of the dissolved salts in solutions or solidification of melts and changes of the substrate temperature.[7,8,10,12,13] They are rather simultaneous processes but they do not necessarily have the same rate.[14]

The spreading time is usually very short depending not only on the droplet size but also on the impact speed, as reported in the literature.[15] It takes usually around 1 ms for a water droplet of about 3 mm in diameter which is spreading on glass to form a first splat (phase c in Figure 1), around 10 ms to form a "crown" shaped splat (phase f in Figure 1), and about 50−70 ms to reach the equilibrium. The impact speed of these large droplets is in the 0.7−2.3 m/s range.[15] In the ESD process, the liquid droplets generated are very small.

The liquid droplets generated in the ESD process are very small. Typically, their size ranges from 2 to 10 μm.[16] Spreading of such small droplets is an even faster process: it takes between 10 μs to 1 ms for a droplet to spread completely.[17,18] Their speed is about 5−10 m/s, with peak values of 20−25 m/s.[19] Furthermore, the small quantity of liquid forms a very thin film that is rapidly stabilized by the stronger effect of the surface tension. Therefore, spreading reaches the equilibrium immediately after the splat arrives at its maximum size.

When impacting a hot surface, large (mm size) droplets may boil or even float on a thin vapor layer and rebound. However, spreading is faster than the heating of the droplet and it spreads to its maximum extent before boiling and evaporation occur.[15] The behavior of small droplets is again different. Individual droplets usually form such a thin layer of liquid that it evaporates almost instantly. It is too thin for boiling centers to develop.

(9) Sivakumar, D.; Nishiyama, H. *Int. J. Heat Mass Transfer* **2004**, *47*, 4469.
(10) Pasandideh-Fard, M.; Chandra, S.; Bhola, S.; Mostaghimi, J. *Int. J. Heat Mass Transfer* **1998**, *41*, 2929.
(11) Pasandideh-Fard, M.; Mostaghimi, J.; Chandra, S. *ILASS-Americas 12th Annual Conference on Liquid Atomization and Spray Systems*, Indianapolis, IN, May 16−19, 1999.
(12) Pasandideh-Fard, M.; Mostaghimi, J.; Chandra, S. *3rd ASME/JSME Joint Fluids Engineering Conference*, San Francisco, CA, July 18−23, 1999.
(13) Pasandideh-Fard, M.; Aziz, S. D.; Chandra, S.; Mostaghimi, J. *Proceedings of the 33rd National Heat Transfer Conference*, Albuquerque, New Mexico, August 15−17, 1999.
(14) Rioboo, R.; Marengo, M.; Tropea, C. *Exp. Fluids* **2002**, *33*, 112.
(15) Bernardin, J. D.; Stebbins, C. J.; Mudawar, I. *Int. J. Heat Mass Transfer* **1997**, *40*, 43.
(16) Perednis, D. Thin film deposition by spray pyrolysis and the application in solid oxide fuel cells. Ph.D. Thesis (Diss. No. 15190), Swiss Federal Institute of Technology, Zürich, 2003.
(17) Shiraz, D. A.; Chandra, S. *Int. J. Heat Mass Transfer* **2000**, *43*, 2841.
(18) Mehdi-Nejad, V.; Ghafouri-Azar, R.; Pasandideh-Fard, M.; Mostaghimi, J. Centre for Advanced Coating technologies web page. http://www.mie.toronto.edu/labs/cact/modelling/modelling.htm.
(19) Olumee, Z.; Callahan, J. H.; Vertes, A. *J. Phys. Chem. A* **1998**, *102*, 9154.

Table 1. Temperature of the Substrate Surface

heating plate temperature (°C)	substrate temperature (°C)
200	146
300	214
400	285
500	359

The purpose of this study is to focus on the very first stages of zirconia coating formation by ESD. The process will be investigated at two different scales. First, at the scale of the individual droplets to describe their spreading and drying and, second, at the larger scale of the coating to understand its formation and evolution. The influence of the major ESD process parameters such as the temperature of the substrate and concentration of salts and additives will be systematically investigated.

Materials and Methods

Zirconia coatings were prepared using a vertical ESD setup similar to that described in the literature.[20,21]

ZrO_2 films were deposited on a heated glass substrate by spraying precursor solutions. Rectangular-shaped 20 × 20 mm and 1 mm in thickness microscope slides were used as substrates. A mixture (40:40:20 vol. %) of diethylene glycol monobutyl ether, $CH_3(CH_2)_3$-$OCH_2CH_2OCH_2CH_2OH$, 99+% (Acros Organics), commonly known as butyl carbytol, water, and ethanol, C_2H_5OH, 99.9% (Prolabo), was used as solvent for zirconyl nitrate hydrate $ZrO(NO_3)_2$·aq (Fluka Chemie). The total concentration of the salt in the solution was 0.04, 0.08, and 0.16 mol/L. Additionally, solutions containing 0.25 and 0.50 wt % of polymer additives have been prepared. Poly(vinyl alcohol) (PVA) 87% hydrolyzed and poly(ethylene glycol) (PEG) of 2000 g/mol molecular weight have been used as polymer additives. In the following, the solvent mixture will be referred to as BWE 442, while the zirconyl nitrate will be referred to as ZN.

Flow rate of precursor solution was 0.5 mL/h, controlled by a Sage M361 syringe pump. The precursor solution was atomized using a positive high voltage from 5 to 8 kV. The nozzle-to-substrate distance was 27 mm. The deposition time used for the spreading experiments is 5 s, while for the coating growth experiments it ranges from 10 s to 10 min. The deposition temperature was ranging from 200 to 500 °C, as measured by a thermocouple placed on the heating plate. The real temperature, measured at the surface of the glass substrate, is given in Table 1. All the temperatures indicated in this paper are heating plate temperatures.

To investigate the thermal decomposition of the zirconyl nitrate, a thermal analysis of the salt has been carried out on a SETARAM TAG 24 symmetrical thermal analyzer, at a heating rate of 3 °C/min, in air.

The morphologies of the splats and the microstructures of the coatings have been analyzed using optical microscopy (Leitz optical microscope with a Sony CCD camera and a Panasonic video printer) and scanning electron microscopy (LEO 440).

(20) Chen, C.; Kelder, E. M.; Jak, M. J. G.; Schoonman, J. *Solid State Ionics* **1996**, *86−88*, 1301.
(21) Chen, C.; Kelder, E. M.; Schoonman, J. *J. Mater. Sci.* **1996,** *31*, 5437.

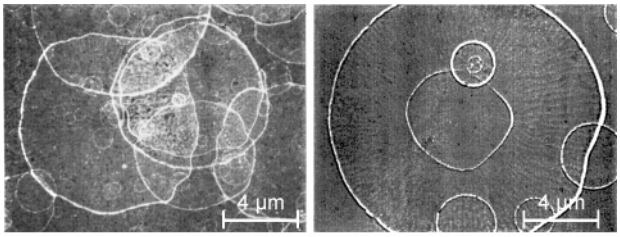

Figure 2. Splats of 0.04 M ZN in BWE 442 at 300 °C, on glass.

Results and Discussion

Spreading and Drying of Droplets in ESD. In this part of the study, a mechanism describing spreading and drying of small droplets of solutions containing ZN as precursor is discussed.

Figure 2 shows two optical micrographs of a solution of 0.04 M ZN in BWE 442 droplets sprayed on glass at 300 °C. Regardless of their size, they all exhibit the same shape, a more or less regular disk with a thick outer border, suggesting a similar spreading mechanism.

The presumed formation mechanism implies that first the droplet spreads completely and very fast, and then the solvent starts to evaporate. Considering the temperature distribution in the liquid layer and in the substrate at the end of the spreading phase,[10,12] the evaporation is likely to be more intense at the border of the splat because of the higher local temperature and the presence of the triple contact point (solid−liquid−vapor). Once started, the evaporation generates a migration of the solution from the center of the splat to the border. This process continues, with the border becoming thicker and thicker, until the heating of the splat raises the temperature of the liquid layer up to the boiling point of the solvents. At this moment, the splat dries almost instantaneously, leaving behind a thin solid film with a thick border.

The hole in the middle of some large droplets, which is shown in Figure 2b, may be the result of the breaking of the fluid layer by the fluid flow at its maximum expansion during spreading. At the newly created inner border, the processes are the same as on the outer border with the solution starting to evaporate. Since the temperature of both the fluid and the substrate is lower in the middle of the splat, the evaporation is less intense and leads to a thinner border.

Influence of the Substrate Temperature. Figure 3 shows optical microscope images of droplets obtained by spraying the same solution of 0.04 M ZN in BWE 442 mixture onto heated glass substrates, at temperatures ranging from 200 to 500 °C.

One can easily observe two different behaviors corresponding to two temperature domains: from 200 to 400 °C (Figure 3a−e), where splats are present, and above 400 °C (Figure 3f), where no indication of spreading is present. From 200 to 400 °C, the same general formation mechanism described above is observed: the droplets are still liquid and spread when they reach the substrate. At 200 °C (Figure 3a), the droplets spread very well and they are cold enough to allow the solution to accumulate on the surface of the substrate and boil. Figure 4 shows trapped bubbles in the thicker part of the deposit. The presence of the bubbles only

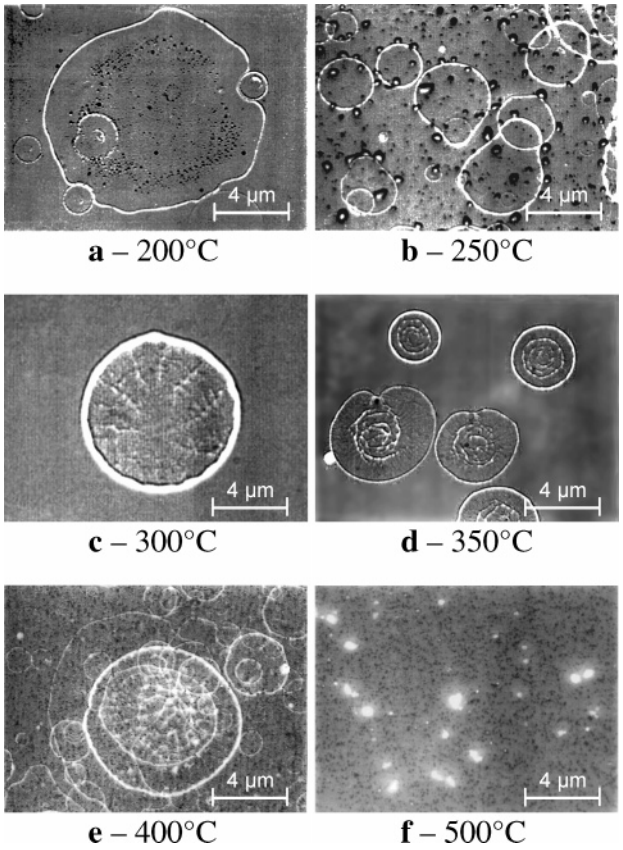

Figure 3. Evolution of the spreading and drying of droplets with the increasing substrate temperature. 0.04 M ZN in BWE 442 on glass substrate. a, 200 °C; b, 250 °C; c, 300 °C; d, 350 °C; e, 400 °C; and f, 500 °C.

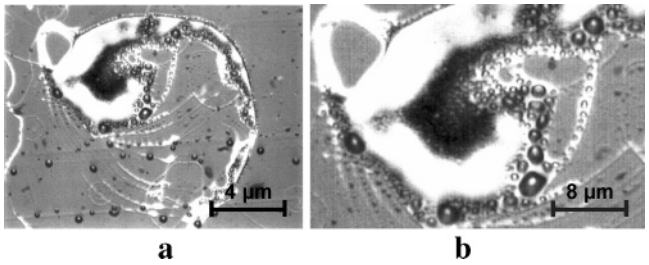

Figure 4. Boiling of solvent in a large accumulation of solution, at 200 °C. a, full picture; b, detail.

on the borders of the successively impacting droplets confirms that this is the hottest area of the splat.

For a substrate temperature of 400 °C (Figure 3e), splats of similar size, but with thinner borders, are observed. This fact suggests that the spreading time remains basically in the same range of magnitude while the time required for the droplet to heat up and dry has significantly decreased. Indeed, at a higher substrate temperature the droplets loose a larger amount of their solvent as a result of the more intense radiative "preheating" during the flight between the needle and the substrate. Therefore, once spread, they heat up and dry faster. This allows only for a limited quantity of solution to migrate and evaporate on the border.

Splats of droplets spread at 300 °C (Figure 2b and Figure 3c), 350 °C (Figure 3d), and 400 °C (Figure 3e) exhibit very fine cracks that are not present at lower temperatures. The equivalent glass surface temperature range (approximately 215−285 °C, see table 1) corresponds to the last stage of the ZN decomposition as previously determined by thermal

Table 2. Air Temperature from the Substrate to the Nozzle

nozzle to substrate distance (mm)	air temperature (°C)
0	354
4	202
10	112
15	87
22	75
32	67

(TG/DTA) analyses. Indeed, almost 80% of ZN is decomposed at this temperature. Hence, the cracks may be the result of the precursor decomposition.

At 500 °C, the droplets lose almost completely their solvent before reaching the substrate. Indeed, the air temperature around a droplet is really high as proved by temperature measurements at several points between the spray nozzle and the substrate (Table 2). Moreover, the residence time of the particle in the hot air is long when a low rate of precursor solution is only 0.5 mL/h. We have to take into account the radiative and convective heat transfer from the substrate to the droplets which is increasing when the substrate temperature is increased. Therefore, the effect of substrate temperature is more significant during the droplets flight than during the impact. Consequently, the dried droplets simply adhere on the surface with no spreading (Figure 3f).

This part of our study shows that the temperature of the substrate does not influence significantly the spreading and drying of the droplets in the ESD as long as they do not dry completely before reaching the substrate. This reduced influence of the temperature can be explained by the fact that spreading itself is much faster than the heating of the droplets on the surface of the substrate, in the temperature range used in our experiments. Of course, we still consider the temperature as a very important factor of the process, but it has a more significant influence on the droplets during their transport toward the substrate rather than after their impact and spreading.

Influence of the Concentration of Salts. A higher concentration of the dissolved salts in a precursor solution would lead to a higher deposition rate in the ESD process, being an easy and reliable way to control layer thickness. Moreover, the concentration of salts is expected to influence the spreading and drying of droplets.

To study the influence of the concentration of the salts, three solutions containing 0.04, 0.08, and 0.16 M ZN have been sprayed on a glass substrate at 400 °C. Optical micrographs of the resulting splats are shown in Figure 5.

As far as the concentration is increased, heterogeneities are developing as shown by Figure 5b and 5c. The larger amount of precursor that decomposes when concentration is increased leads to larger mechanical stresses in the dried splat and consequently to an increased number of defects.

Indeed, SEM images of 0.04 and 0.08 M ZN confirm the presence of an increased amount of solid matter in the center of the splats and a somehow larger number of little droplets or even dried particles on the 0.08 M sample compared to the 0.04 M ZN (Figure 6).

The presence of small droplets is in agreement with the decrease of the atomized droplet diameter with the increase of the concentration of the salts. Different models are available in the present literature to describe the dependence between the droplet diameter and the properties of the solution in electrostatic atomization. They all are in good agreement with the fact that the diameter of the droplet is proportional with the inverse of the conductivity of the solution. Since the conductivity is proportional with the concentration of salts, a solution of a higher concentration will yield smaller droplets.

Influence of the Additives. Additives, as PEG or PVA, are expected to modify the properties of the solutions, with a possible effect on the spreading and drying of droplets. It is also likely that polyalcohols will influence the precipitation of the salts, delaying and slowing down the solidification by inhibiting the effect of crystallization centers.

It is well known that when PEG is added to an aqueous solution, it is expected to reduce the surface tension and increase the viscosity. Both effects become stronger when the polymer chain length and solution concentration are increased. Regarding the effect of the PEG concentration, the decrease of the surface tension is very fast for concentrations up to 3 wt % and then attenuates at larger PEG concentrations while the viscosity of solution is continuously increasing as the PEG concentration is increased. In other words, a relatively concentrated solution has a slightly lower (1.3 times) surface tension compared to a diluted one, but it is much more viscous (50 times).[22] For alcohol containing solutions, which have an intrinsic surface tension lower than pure water, this effect is even more significant.

In our experiments, solutions of 0.08 M ZN in BWE 442 containing small amounts of PEG (0.5 wt % to the mass of the solution) have been sprayed onto a glass substrate heated at 400 °C. The effect was significant, as shown in Figure 7.

The most obvious change in spreading behavior was observed in the larger droplets deposited at 200 °C. More opaque and homogeneous splats with concentric rings are obtained, in contrast to the clearer ones obtained from the solution without polymer additives. Two effects are to be considered to explain this behavior. First, the solvents evaporate slower in the presence of the polymer because of the interaction with the polymer itself. Indeed, the boiling point of the solution increases. The second and the key effect is that the actual polymer concentration is continuously increasing as far as the solvents evaporate. Considering the influence of the polymer concentration described above, a PEG added splat will have a lower surface tension and a continuously increasing viscosity compared to the one without PEG. This effect and the increased boiling point allow the splat to pass through a longer and delayed spreading process, with more intermediate steps, before reaching the spreading equilibrium. A certain number of such intermediate steps are possible during drying at lower substrate temperatures such as 200 °C (Figure 7b). In this case, a ring of solid matter is generated at the outer border after each step. Only one step is achieved during the much faster evaporation at 400 °C (Figure 7d). The effect is significant enough for the spreading and drying/precipitation to become simultaneous processes.

(22) *CARBOWAX - Polyethylene Glycols and Methoxypolyethylene Glycols Data Sheet*; Dow Chemical Co., August 2002.

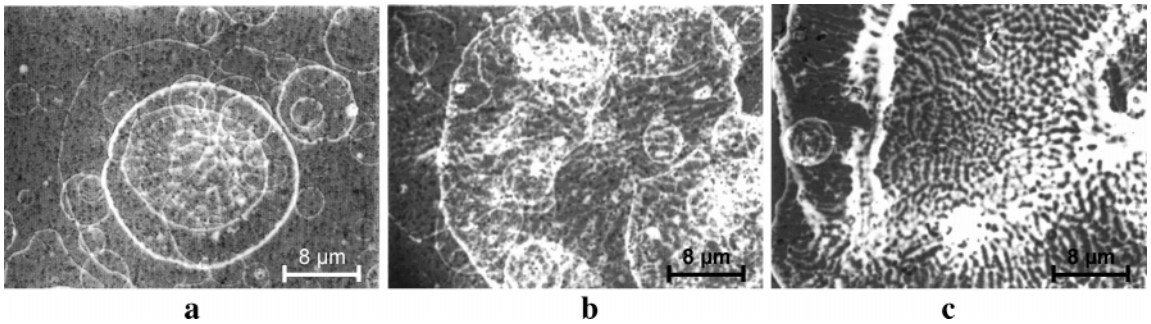

Figure 5. Evolution of the splats morphology when ZN concentration is increased. a, 0.04 M; b, 0.08 M; c, 0.16 M.

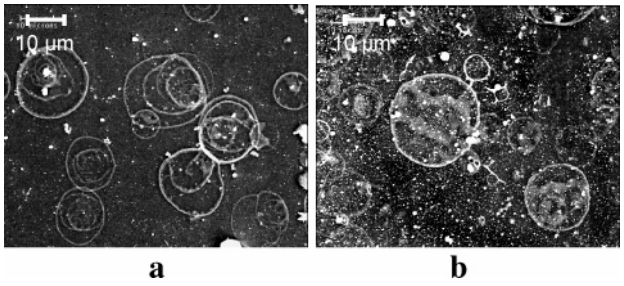

Figure 6. SEM micrographs showing the effect of the ZN concentration. a, 0.04 M; b, 0.08 M.

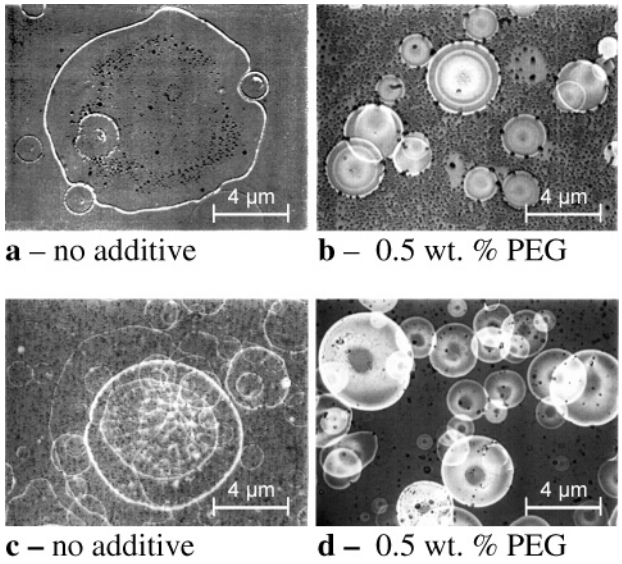

Figure 7. The effect of adding 0.5 wt % of PEG 2000 on droplet spreading and drying for 0.08 M ZN in BWE 442 deposited on glass at 200 °C (a and b) and 400 °C (c and d). Pictures a and c are given for reference.

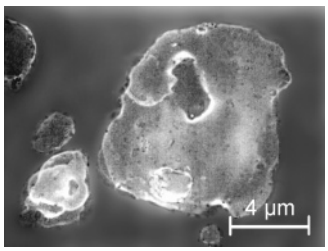

Figure 8. The effect of adding 0.5 wt % of PVA on droplet spreading and drying for 0.08 M ZN in BWE 442 on glass at 400 °C.

Adding 0.5 wt % PVA results in an even lower surface tension and in a very irregular splat shape at 400 °C (Figure 8).

The Mechanism of the Coating Formation. To understand the growth of the coating in its early stages, several series of very short coating experiments have been conducted. First, six ZN coatings were deposited on a glass substrate at 400 °C from a distance of 27 mm, for 10 s and 1, 3, 5, 8, and 10 min, respectively. The 0.08 M ZN in BWE 442 solution has been used as precursor. The microstructure of the coatings is shown in Figure 9.

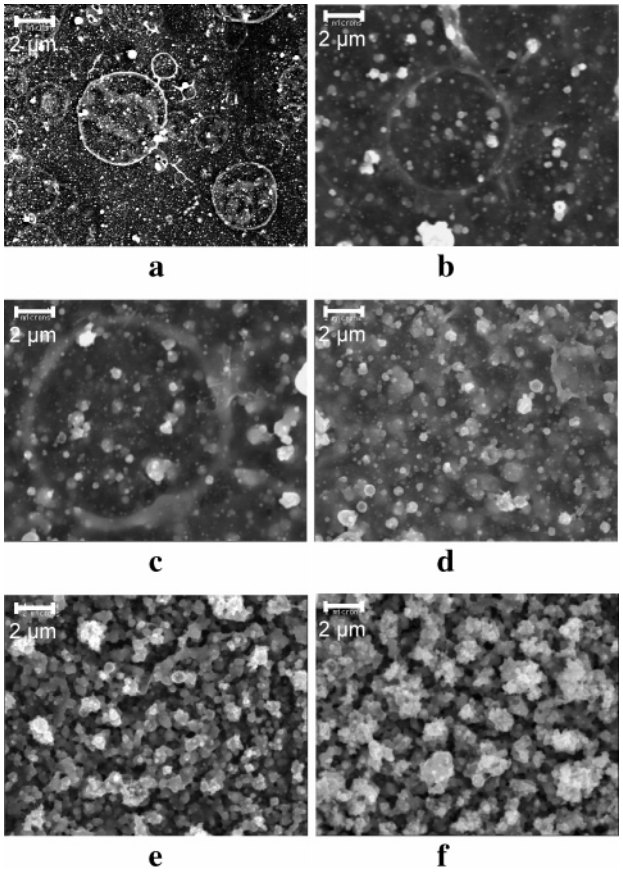

Figure 9. SEM observations showing the time evolution of the ZN coating on glass at 400 °C (0.08 M ZN in BWE 442). a, 10 s; b, 1 min; c, 3 min; d, 5 min; e, 8 min; and f, 10 min.

At 400 °C, the aerosol consists of a mixture of liquid droplets and solid particles. The observations when the deposition time is increased suggest that the growth of the coating is a two-stage process: the first one during the first 3 min and a second one after 3 min. During the first stage, corresponding to Figure 9a−c, a continuous layer of salt is forming on the surface of the substrate. This continuous layer is the result of liquid droplets spreading directly onto the substrate. Simultaneously, the solid particles are either incorporated in the layer or appear on the surface of the coating. We can easily distinguish the splats of individual

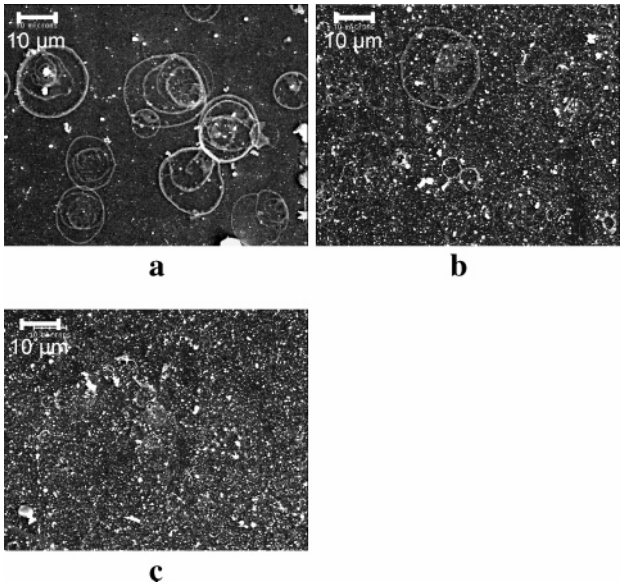

Figure 10. SEM observations of early stages of a ZN coating on glass at 400 °C (0.04 M ZN in BWE 442). a, 10 s; b, 1 min; c, 3 min.

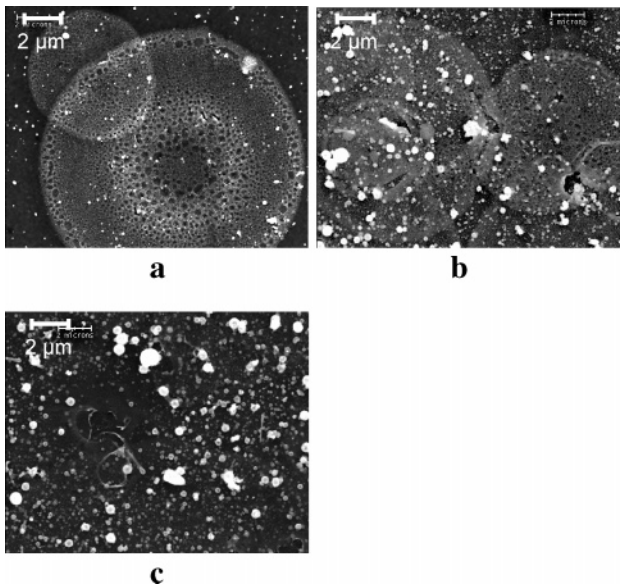

Figure 11. SEM observations of early stages of a PEG added ZN coating on glass at 400 °C (0.08 M ZN in BWE 442 with 0.5 wt % PEG). a, 10 s; b, 1 min; c, 3 min.

droplets after a few seconds of deposition as shown in Figure 9a and Figure 10a. However, these splats are no longer visible on SEM images after longer deposition times (after 3 min in our experiments, Figure 10c).

The same remarks are valid for a 0.5 wt % PEG added solution of 0.08 M ZN in BWE 442. The splats are very well visible after 10 s (Figure 11a) but cannot be distinguished after 3 min of deposition (Figure 11c).

This suggests that, if the deposition time is long enough, the overlapping splats do not dry completely between two successive droplet impacts. The splats cannot reach their final dried shape, as described previously in this work, and additionally a continuous, thin layer of liquid forms on the surface. This liquid layer may be responsible for the healing of surface defects observed in individual splats but not on the final coating surface (Figure 11a compared to Figure 11c).

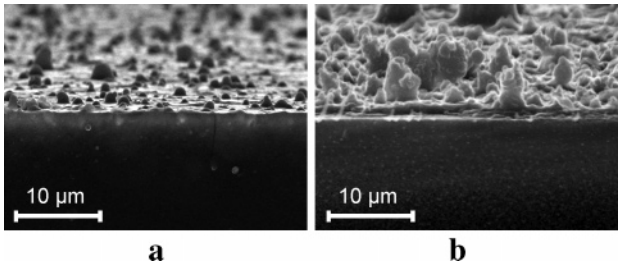

Figure 12. Cross sections of the ZN coating on glass at 400 °C (0.08 M ZN in BWE 442). a, 3 min; b, 8 min.

As far as the process continues, the incoming solid particles and droplets preferentially land on the top of already existing solid particles because the later ones act as concentrators of the electrical field lines at the surface of the substrate (phenomenon already mentioned by Chen et al.).[23] Hence, an increased roughness of the coating is observed. This intermediate phase is shown in Figure 9d. Then, after 5−10 min from the beginning of the coating process, the surface morphology of the layer becomes more and more rough and porous, as shown in Figure 9e and 9f. This increased roughness is the result of the particle agglomeration due to the preferential landing of dried or liquid droplets. It follows that the second stage of the film growth is dominated by the preferential landing.

Figure 12 shows SEM micrographs of cross sections for coatings obtained after 3 and 8 min (corresponding to Figure 9c and 9e).

Many solid particles are present on top of the dense layer after 3 min (Figure 12a) and a porous bilayer starts to form after 8 min of coating (Figure 12b).

The whole process may be seen as a simultaneous growing of two layers: one is formed by the liquid droplets spreading on the surface and the other one by the solid particles stacking up as they arrive on the substrate. The stack of particles, being more porous, grows up faster and becomes the determining factor for the coating microstructure shortly after the beginning of the deposition process. Figure 13 schematically shows this mechanism.

The growth of a porous layer during the later stages of the deposition process is sped up by preferential landing of droplets and solid particles on the highest points of the layer surface. This leads to the formation of columnar or coral-like structures, as shown in Figure 9f, and not to a homogeneous distribution of the porosity.

This work has been focused on the systematic study of the formation of a coating of pure ZrO_2 starting from a precursor solution of ZN in BWE. Furthermore, it is possible to obtain dense films in different experimental conditions and to use a different precursor salt and solvent. For instance, by spraying a solution of 0.1 M zirconium acetylacetonate + YCl_3 in butyl carbytol−EtOH 1:1 vol, a dense coating was successfully obtained as shown in Figure 14. The presence of a liquid layer on the top of the forming coating is probably at the origin of this dense morphology.

Influence of the Substrate Temperature. The substrate temperature is the main controlling factor of the growth

(23) Chen, C. Thin-Film Components for Lithium-Ion Batteries. Ph.D. Thesis, Delft University of Technology, 1998.

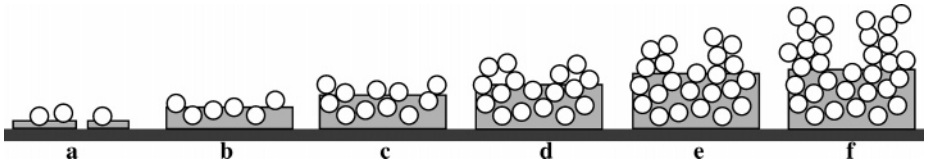

Figure 13. Layer growth mechanism. Steps a−f correspond to images a−f in Figure 9.

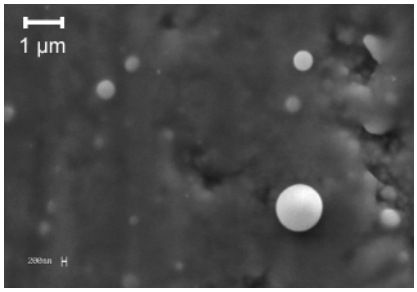

Figure 14. Coating of 0.1 M Zirconium acetylacetonate + YCl_3 in butyl carbytol−EtOH 1:1 vol at 400 °C.

mechanism. In this part, layers were deposited at lower temperatures (200 and 300 °C) using a lower concentration (0.04 M) to investigate the formation of the coating in the case. Indeed, the decrease of deposition temperature and concentration prevents the formation of solid particles during the droplet transport. The solvent mixture and the experimental setup were not changed. The resulting microstructures are shown in Figure 15.

At 200 °C, a dense layer without solid particles was obtained, even after 10 min. However, at such a lower temperature the solvent does not evaporate at a rate high enough. Therefore, a large quantity of solvent evaporates at the end of the deposition process leading to a lot of stress and to the cracking of thicker layers (10-min coating, Figure 15e). At 300 °C, dried particles are present and they are visible after 1 min (detail in Figure 15b). They finally lead to a porous microstructure. Similarly, at 400 °C a porous morphology due to dried droplets develops as already shown in Figure 10b and 10c.

Therefore, the evolution of the layer in the later stages strongly depends on the substrate temperature. A higher temperature leads to drier droplets before the impact and therefore allows the occurrence of uneven points on the surface. This further enhances the preferential landing effect and the formation of a coral-like porous structure. A lower temperature prevents the formation of porous coatings but may lead to drying cracks at the end of the process. Therefore, an optimal temperature should be found between these limits. Since cracks are less desirable than a slight amount of particles, higher deposition temperatures should be considered.

Influence of Additives. As mentioned in the previous part, we have added polymers to the precursor solutions to improve spreading and drying of droplets. 0.25 wt % and 0.5 wt % of PVA and 0.5 wt % of PEG 2000 have been added to solutions of 0.08 M ZN in BWE 442. Coatings were deposited at 400 °C on glass for 1, 5, and 10 min (see Figure 16).

The addition of polymers seems to degrade the quality of the coatings. After 1 min of deposition, the addition of PVA leads to a large amount (Figure 16d−g) of surface irregularities, while the addition of PEG has no significant effect (Figure 16j). Comparing the time evolution of the four samples, a clear change of the microstructure is observed with appearance of cracks in 0.5 wt % PVA and a growth of coral-like microstructure in all other cases as shown, respectively, by Figure 16i and Figure 16l.

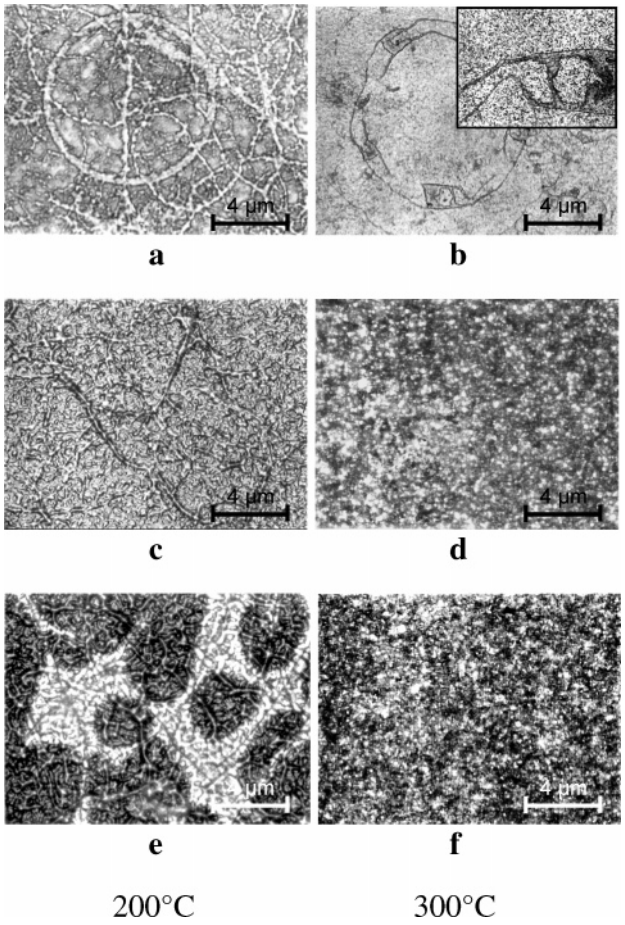

Figure 15. Optical microscope images of 0.04 M ZN coatings (0.04 M ZN in BWE 442) on glass at 200 and 300 °C, respectively. a, b: 1 min; c, d: 5 min; e, f: 10 min.

The effects of these two additives may be explained by the decrease of the surface tension of the precursor solutions. This change in the surface tension results in smaller droplets, as predicted by eq 1[23] and already detailed in the first part of this paper.

$$d \approx \sqrt[3]{\frac{\gamma \epsilon_0^2}{\sigma^2 \rho}} \qquad (1)$$

where γ is the surface tension, ϵ_0 is the electrical permittivity, ρ is the density, and σ is the conductivity of the solution.

Droplets containing more dissolved matter, such as added polymers or high concentration of precursor salts, are expected to dry faster compared to the ones with no additives.

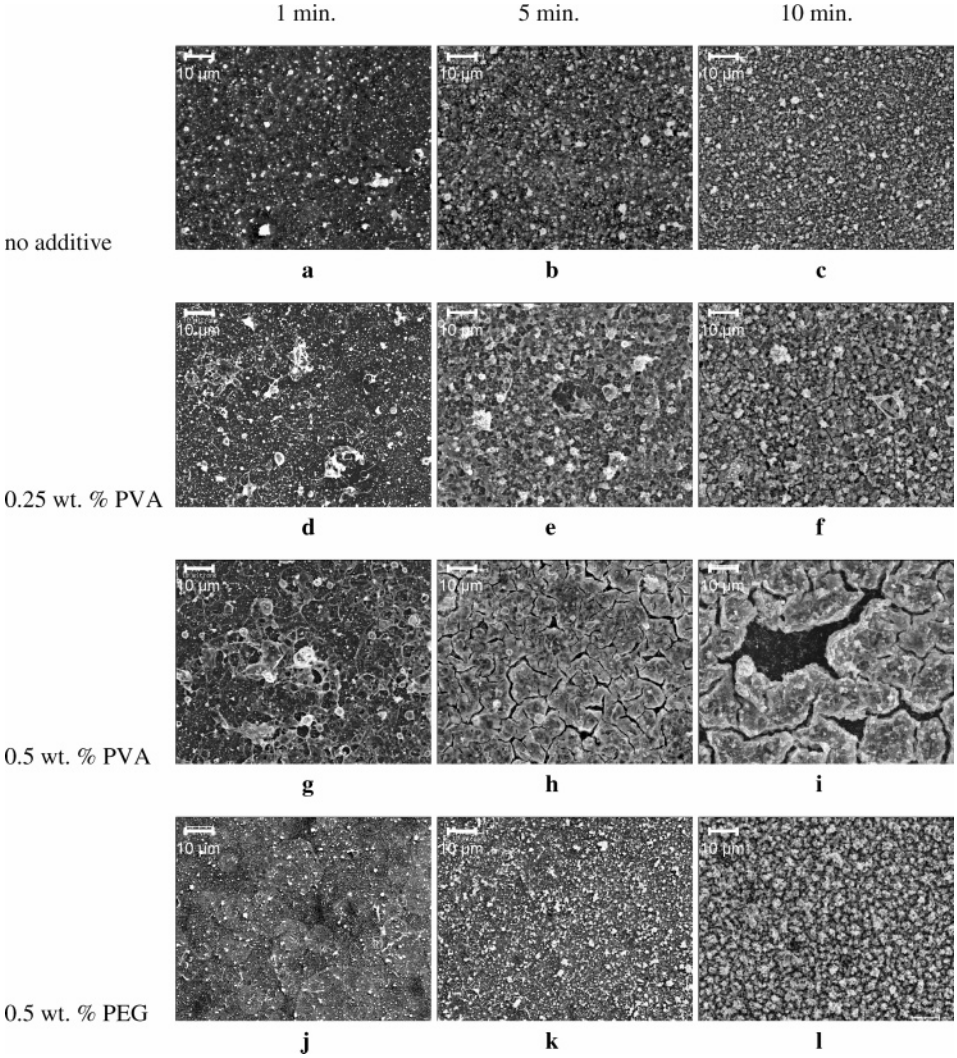

Figure 16. SEM observations of the evolution in time of coatings of 0.08 M ZN in BWE 442 containing additives (0.25 wt % PVA, 0.5 wt % PVA, and 0.5 wt % PEG).

It follows that in droplets with additives, a larger number of dried particles will occur and they will act as centers for the preferential landing on the surface of the coating. Therefore, the addition of a polymer to precursor solutions would generally lead to a larger roughness or a coral-like structure for longer deposition time, as shown by the coatings containing PEG and 0.25 wt % PVA after 10 min.

The different aspect of the 0.5 wt % PVA containing coating may be due to the melting of the polymer and to its relatively low T_g. PVA has a T_g of approximately 60−70 °C and melts at approximately 180 °C.[24] Therefore, the droplets remain in a highly viscous liquid state over a large range of temperatures and, correspondingly, for a longer time. A higher quantity of liquid is still present on the substrate during the deposition and may explain the absence of the coral-like microstructure (no accretion points available on the surface) as well as the severe cracking observed on these coatings.

Influence of the Concentration of Salts. Three different solutions of 0.04, 0.08, and 0.16 M of ZN in BWE 442 have been deposited on glass substrates at 400 °C for 1, 5, and 10 min, respectively. The results are shown in Figure 17.

An increasing roughness and porosity are detected when the concentration of salts and deposition time are increased. After a short deposition time, the difference between the three samples is small: the 0.16 M sample exhibits larger dried droplets. The difference becomes more visible after 5 min: an increased roughness of the 0.08 M sample and a very well developed coral-like structure on the 0.16 M sample. After 10 min, the coral-like structure is present in all the samples, the size of the surface features becoming larger and larger as the concentration is increased. In fact, higher concentration is expected to lead to smaller atomized droplets according to eq 1 as discussed previously in this paper. Smaller droplets are subject to preferential landing; therefore, the coral-like structure develops earlier and grows faster when the concentration of the precursor solution is increased. Hence, the coral-like agglomerations are thicker and separated by larger spaces. A "scaled-up" microstructure results as shown in Figure 17i.

A second consequence of an increased concentration is that droplets get dried faster. This may be an explanation for the larger dried droplets observed in the early stages of

(24) Polyvinyl Alcohol Characteristics, ERKOL S. A. web site. http://www.erkol.com/eng/Characteristics.htm.

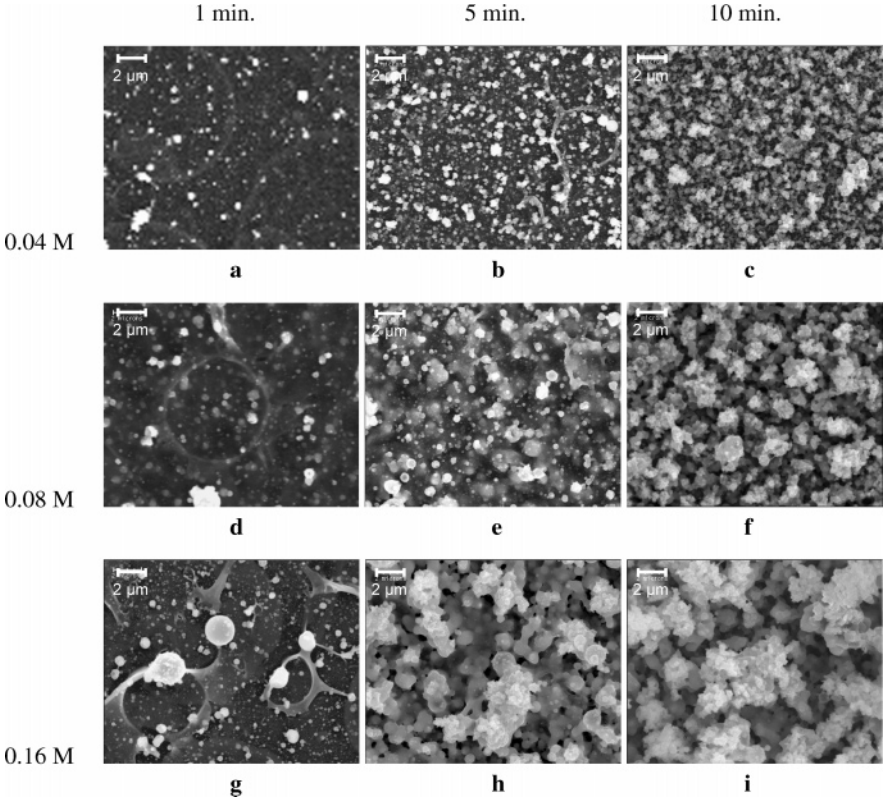

Figure 17. SEM observations of coatings of ZN in BWE 442 for three different concentrations and when deposition time is increased.

the deposition process on the 0.16 M sample (Figure 17g). On one hand, this effect reduces the number of spreading droplets, on the other hand, larger particles are present on the surface of the coating early during its formation and may act as agglomeration points.

This work brings a new insight in the formation of ESD coatings with different microstructures. In this context, studies on the synthesis of thin dense YSZ coatings are in progress. They may finally contribute to the preparation of thin YSZ layers for applications as SOFC electrolytes.

Conclusions

This study has been focused on the first stages of the formation of a zirconia coating by electrostatic spray deposition (ESD).

The process of the ESD coating formation can be described in two successive stages. During the first one—very short, taking the first approximately 30 s—the droplets come into direct contact with the hot substrate. The spreading and drying of individual droplets control this stage. During the second one, the formation of the coating depends on the evaporation of the solvent mixture on the surface of the substrate and during the transport of the droplets. If the evaporation rate is low, a certain amount of liquid arrives on the substrate. In the case of a small excess of arriving liquid, surface defects that appeared during the initial step may be healed, but a too large amount of liquid can cause cracking of the layer in the final drying stage. In optimal conditions, a part of the droplets may dry during transport but they are incorporated into the forming coating. If the number and the size of the dried droplets are too large, the process—mainly controlled by the preferential landing—leads to the formation of a porous, coral-like structure.

Substrate temperature, salt concentration, and presence of polymer additives have a significant influence on the duration and evolution of each stage.

The influence of the substrate temperature becomes more effective during the formation of the coating, which is conducted by preferential landing, than for the initial spreading and drying step. Dense, cracked films and porous, not cracked films can be obtained in the temperature domain ranging, respectively, from 200 to 500 °C.

The concentration of salts changes the final aspect of the splats and the microstructure of the coating. Indeed, a higher concentration stimulates the precipitation of salts and the formation of heterogeneous solid particles, with the development of a porous, coral-like structure. Therefore, a lower concentration would be more suitable for the formation of a dense coating.

Additives, such as PVA and PEG, reduce the surface tension of the solutions and increase their conductivity. Both influences converge to the same effect: droplet size is decreased and the formation of porous structures by accretion is promoted. They proved to have the most significant influence on the spreading stage of all the three parameters investigated in this study. Also, the melting of PVA has completely changed the porous microstructure of the thick layer. During the later stage of the coating process, it favors the formation of a dense but cracked layer.

CM048341P